preliminary design, where the basic structural configurations will be established.

Sandwich structures, of which the truss-core sandwich has been selected as representative, are shown to be very efficient load-carrying members for all loading-component combinations treated in this article, except as wide columns—particularly at low to moderate values of the various loading indexes.

Cross-rolled beryllium sheet is the most efficient material for all configuration-loading-component combinations investigated, when elastically stressed in the lower temperature range. In applications involving plastic stresses, beryllium is competitive with the so-called high-strength materials.

The validity of small-deflection theory for predicting the behavior of axially compressed, long, truss-core sandwich circular cylindrical shells has been verified for a portion of the practical design range by some independently conducted tests. Further experimental verification of the theoretical minimum weight analyses presented here is required, particularly for structures such as the axially compressed cylinder, where controversy exists over the proper theory for predicting their buckling behavior. Minimum weight studies of other stiffened structural components, such as conical shells and spherical caps, are needed. In addition, the minimum weight of structures under combined loading is of interest and should be determined.

References

[1] Zahorski, A., "Effects of material distribution on strength of panels," J. Aeronaut. Sci. 2, 247–253 (1944).

[2] Farrar, D. J., "Design of compression structures for minimum weight," J. Roy. Aeronaut. Soc. **47**, 1041–1052 (1949).

[3] Shanley, F. R., *Weight-Strength Analysis of Aircraft Structures* (McGraw-Hill Book Co., New York, 1952), Chap. 2.

[4] Gerard, G., *Minimum Weight Analysis of Compression Structures* (N.Y.U. Press, New York, 1956).

[5] Catchpole, E. J., "Optimum design of compression surfaces having unflanged integral stiffeners," J. Roy. Aeronaut. Soc. **58**, 765–768 (1954).

[6] Crawford, R. F. and Stuhlman, C. E., "Minimum weight analyses for truss-core sandwich cylindrical shells under axial compression, torsion or radial pressure," Lockheed Rept. 2-47-61-2, ASTIA AD-267625, Sunnyvale, Calif. (1961).

[7] Stein, M. and Mayers, J., "Compressive buckling of simply supported curved plates and cylinders of sandwich construction," NACA TN-2601 (1952).

[8] Crawford, R. F., Burns, A. B., and Tilcens, L. K., "Minimum weight analyses and design procedures for flat, truss-core sandwich panels," Lockheed Rept. LMSD-704009, ASTIA AD-250810, Sunnyvale, Calif. (1960).

[9] Anderson, M. S., "Local instability of the elements of a truss-core sandwich plate," NASA TR R30 (1959).

[10] Timoshenko, S., *Theory of Elastic Stability* (McGraw-Hill Book Co., New York, 1936), p. 158.

[11] Eakin, E., "Honeycomb cylinder tests," Douglas Aircraft SM-37719, Santa Monica, Calif. (1961).

[12] Crawford, R. F. and Burns, A. B., "Strength, efficiency, and design data for beryllium structures," Aeronaut. Systems Div. TR 61-692, Wright-Patterson Air Force Base, Ohio (1962).

[13] Nickell, E. H. and Crawford, R. F., "Optimum ring stiffened cylinders subjected to uniform hydrostatic pressure," Soc. Automotive Engrs. Preprint 578F (1962).

[14] Seide, P. and Stein, M., "Compressive buckling of simply supported plates with longitudinal stiffeners," NACA TN-1825 (1949).

APRIL 1963 AIAA JOURNAL VOL. 1, NO. 4

Conical Segment Method for Analyzing Open Crown Shells of Revolution for Edge Loading

ROBERT R. MEYER* AND MARILYN B. HARMON†
Douglas Aircraft Company Inc., Santa Monica, Calif.

A solution, accurate, rapid, simple enough for design use, and valid for all regions, has been obtained for the stress distribution and influence coefficients for a variable thickness shell of revolution formed by a generator of arbitrary shape. The shell is subdivided into a series of equivalent conical segments whose individual thicknesses are the local segment average. Conditions of continuity then are applied at the boundaries of each conical segment to evaluate the indeterminate edge shears and moments using digital equipment. Influence coefficient comparisons for a wide range of shell geometries are made between the cone solution and solutions by other methods from the literature and show agreement within 4%. The cone solution reciprocity relations are shown to be valid to five significant figures. Limiting conditions indicate that good approximations of the influence coefficients and the stresses can be obtained by using 10 cones in most cases.

Nomenclature

E = modulus of elasticity
ν = Poisson's ratio
t = thickness
Δz = altitude of a truncated conical segment
R = radius of curvature of the median surface of the cone measured in the truncating plane
α = angle between the axis of revolution and the generatrix of the conical segment
X_i = load or moment applied to an edge of a conical segment
δ_{ik} = deflection at i in the direction of load X_i due to a unit load at k (displacement or rotation), influence coefficient
a = distance from the shell axis of rotation to the center of the radius of curvature for a toroidal shell
b = maximum shell cross-section dimension, i.e., toroidal radius or major axis of an ellipse
Q_s = shear force on the meridian plane
N_s = normal force on the meridian plane
M_s = bending moment on the meridian plane

Received by IAS June 5, 1962; revision received January 18, 1963. The authors wish to thank Barbara Freeman and Ralph Kahn of the Space Computing Engineering Section, Douglas Aircraft Company Inc. for programming the equations in this article for the IBM 7090 computer.

* Space Strength Section, Missile and Space Systems Division.
† Space Strength Section, Missile and Space Systems Division.

N_θ = normal force on the plane perpendicular to the meridian plane (hoop)
M_θ = bending moment on the plane perpendicular to the meridian plane (hoop)

Introduction

FOR many years investigators have directed their activities toward solving the shell equations to obtain the edge solutions for various shells of revolution.[1, 7-9] Limiting sequences used to obtain a solution can be defined in a variety of ways. The sequence may be defined, for example, by a series, by a finite difference mesh, or by a numerical integration interval where the mesh or interval subdivision defines the sequence. In this paper, the sequence is defined by a cone subdivision. The rapidity of approach to a limit in any case will depend upon in which stage of the analysis the sequence is defined. It is believed that the rapidity of the approach to a limit of the conical solution presented here lies basically in the fact that the sequence is defined at a later stage in the analysis than for a finite difference grid or numerical integration interval where magnification of the sensitivity to the interval may appear in the convergence of the final results.

The solution for any number of cones as proposed here can be programmed for a digital computer. A simple input of geometry and loading quickly will yield the deflection influence coefficient matrix and bending stress distribution for use in thin shell design. The shell of revolution, formed by a generator of arbitrary shape, can have any meridional thickness variation, and it is possible to take into account a change of material or material properties as the shell is traversed from crown to base.

The original shell is considered to be a limiting sequence of circular conical shell frustums that, when assembled together with conditions of continuity satisfied, closely resemble the original shell (Fig. 1). Each conical segment has constant material properties and thickness, the average of the material properties and the thickness variation in the original shell region represented by that conical segment. Many short cones are cut in regions of rapidly changing geometry or material properties, whereas in less disturbed regions a few cones will yield a satisfactory solution. The individual cone solution is shown to be rigorously valid for all ranges of opening angle from a cylinder to a flat plate (Appendix A).

Deflection Influence Coefficients

A comparison of the cone solution deflection influence coefficients with the deflection coefficients for toroids, ellipsoids, and shells of negative curvature, derived by other methods,[3-5] shows a maximum of 4% difference for the three numerical examples given (Tables 1–3). This percentage range generally held for other numerical examples compared with the forementioned literature sources.

Using the reciprocity relations [Appendix A, Eq. (A10)], the check matrix δ_{ik} $(i,k = 1, 2, 3, 4)$ for 15 cones and $E = 10 \times 10^6$ for the toroidal example yields the following values:

+0.00083963316	−0.00044246235
−0.00044246309	+0.0011778462
−0.000082054413	+0.000081082908
−0.000067329702	+0.00010251960

Similar matrix reciprocity checks for other numerical examples using the cone solution exhibit five digit accuracies comparable to those shown here (i.e., δ_{12} compared to δ_{21}, etc., in the foregoing). The authors are not aware of any other methods exhibiting comparable accuracies in the reciprocity relations.

It is of interest to investigate the manner in which the deflection influence coefficients approach a limit as the number of cones is increased. The main diagonal terms for the toroidal example[3] are shown in Fig. 2. The rapid approach of the coefficients to limiting values suitable for design is typical for the various shell geometries analyzed.

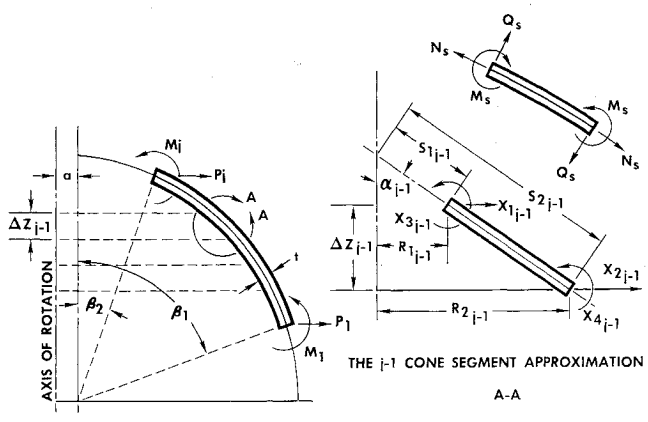

Fig. 1 A toroidal shell illustrating the use of the cone approximation

Stress Distributions

Comparison data for bending stress distributions of unpressurized shells were unavailable in the unclassified literature.‡ It is of interest to note, however, the effect of the number of cones used to approximate the shell upon the convergence of the stress values to a limiting case resulting from a fine lumping of cones. An example of an ellipsoidal shell using 20 cones as the limiting case is shown in Fig. 3, which was typical of comparisons made for other shell geometries.

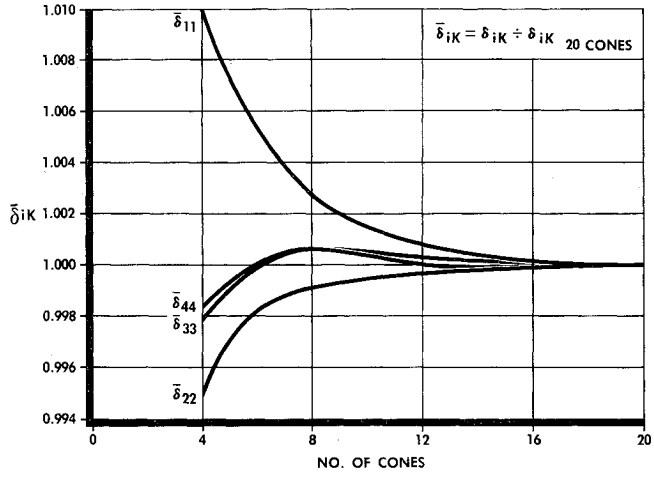

Fig. 2 The variation of the influence coefficient (normalized to the 20-cone solution) for the toroidal shell[3] example

−0.000082054375	−0.000067329376
+0.000081083109	+0.00010251973
+0.000013781843	+0.0000075268471
+0.0000075269255	+0.000013740710

Conclusions

Stress analysts have needed a rapid method of obtaining good approximations of the influence coefficients and bending stress distributions for edge-loaded shells for which exact solutions are not available. The cone solution presented here, using a computer such as the IBM 7090, quickly will yield in-

‡ See Appendix B.

fluence coefficients and stresses for any thin shell of revolution within design accuracy. The limiting cases of any governing equations are the flat plate and the cylinder, thus permitting the analysis of a wide range of shell geometries. Variable thickness and variations of material can be included in the analysis.

Appendix A

Individual Cone: Derivation

The cone problem consists of solving a fourth-order differential equation with four constants of integration for each of the four different boundary conditions. Splitting the fourth-order equation into a pair of second-order equations (1), one obtains, using the notation defined by Fig. 1,

$$L_c(sQ_s) \pm i\lambda^2 sQ_s = 0 \tag{A1}$$

where

$$L_c = s\frac{d^2(\cdots)}{dS^2} + \frac{d(\cdots)}{dS} - \frac{(\cdots)}{S}$$

Using the transformation $\eta = x(i)^{1/2} = 2\lambda(i)^{1/2}\cdot(s)^{1/2}$, the solution of the cone problem then depends upon the solution of

$$\frac{d^2(sQ_s)}{d\eta^2} + \frac{1}{\eta}\cdot\frac{d(sQ_s)}{d\eta} + \left(1 + \frac{4}{\eta^2}\right)(sQ_s) = 0$$

This solution is given by[1]

$$sQ_s = C_1[ber\ x - (2/x)bei'\ x] + C_2[bei\ x + (2/x)ber'\ x] + C_3[ker\ x - (2/x)kei'\ x] + C_4[kei\ x + (2/x)ker'\ x] \tag{A2}$$

where

E = modulus of elasticity
ν = Poisson's ratio
$\lambda 4 = [12(1 - \nu^2)/t^2]\cot^2\alpha$
$x = 2\lambda(s)^{1/2}$

All the other desired quantities, M, N, and δ, depend upon various linear combinations of Eq. (2) and its derivatives, i.e., a suitable combination of the constants of integration. A double subscript notation is adopted for the constants of integration C_{pk} such that the first subscript p indicates a constant of integration number $p = 1, 2, 3, 4$; and the second subscript k, where $k = 1, 2, 3, 4$, corresponds to the subscript of one of the unit edge loads, $X_k = 1$, to identify the loading condition. To simplify the solution, the following combinations of Kelvin functions will be defined:

$$\begin{aligned}
A_{1x} &= ber\ x - (2/x)bei'\ x \\
B_{1x} &= x\ bei'\ x - 2(1-\nu)[bei\ x + (2/x)ber'\ x] \\
A_{2x} &= bei\ x + (2/x)ber'\ x \\
-B_{2x} &= x\ ber'\ x - 2(1-\nu)[ber\ x - (2/x)bei'\ x] \\
A_{3x} &= ker\ x - (2/x)kei'\ x \\
B_{3x} &= x\ kei'\ x - 2(1-\nu)[kei\ x + (2/x)ker'\ x] \\
A_{4x} &= kei\ x + (2/x)ker'\ x \\
-B_{4x} &= x\ ker'\ x - 2(1-\nu)[ker\ x - (2/x)kei'\ x]
\end{aligned} \tag{A3}$$

The solution for the shear resultant Q_s then can be represented by

$$sQ_s = C_{1K}A_{1x} + C_{2K}A_{2x} + C_{3K}A_{3x} + C_{4K}A_{4x} \tag{A4}$$

Similarly, the solution for the meridian moment resultant is given by

$$x^2M_s/2 = C_{1K}B_{1x} + C_{2K}B_{2x} + C_{3K}B_{3x} + C_{4K}B_{4x} \tag{A5}$$

The boundary conditions are

$$\begin{aligned}
K = 1 \quad & X_1 = 1 = \frac{Q_s}{\cos\alpha} \quad && X_2 = X_3 = X_4 = 0 \\
K = 2 \quad & X_2 = 1 = -\frac{Q_s}{\cos\alpha} \quad && X_1 = X_3 = X_4 = 0 \\
K = 3 \quad & X_3 = 1 = -M_s \quad && X_1 = X_2 = X_4 = 0 \\
K = 4 \quad & X_4 = 1 = M_s \quad && X_1 = X_2 = X_3 = 0
\end{aligned}$$

If the values of A_{px}, B_{px} at $x = x_1, x_2$ are denoted by A_{p1}, A_{p2} and B_{p1}, B_{p2}, the boundary conditions may be represented by the following matrix:

$$\begin{bmatrix} A_{11} & A_{21} & A_{31} & A_{41} \\ A_{12} & A_{22} & A_{32} & A_{42} \\ B_{11} & B_{21} & B_{31} & B_{41} \\ B_{12} & B_{22} & B_{32} & B_{42} \end{bmatrix}\begin{bmatrix} C_{11} & C_{12} & C_{13} & C_{14} \\ C_{21} & C_{22} & C_{23} & C_{24} \\ C_{31} & C_{32} & C_{33} & C_{34} \\ C_{41} & C_{42} & C_{43} & C_{44} \end{bmatrix} =$$

$$\begin{bmatrix} S_1\cos\alpha & 0 & 0 & 0 \\ 0 & -S_2\cos\alpha & 0 & 0 \\ 0 & 0 & -(x_1^2/2) & 0 \\ 0 & 0 & 0 & x_2^2/2 \end{bmatrix} \tag{A6}$$

In terms of the functions

$$\begin{aligned}
D_{1x} &= bei\ x + (2/x)ber'\ x \\
E_{1x} &= -xber'\ x + 2(1+\nu)ber\ x - (4/x)(1+\nu)bei'\ x \\
-D_{2x} &= ber\ x - (2/x)bei'\ x \\
E_{2x} &= -xbei'\ x + 2(1+\nu)bei\ x + (4/x)(1+\nu)ber'\ x \\
D_{3x} &= kei\ x + (2/x)\ ker'\ x \\
E_{3x} &= -xker'\ x + 2(1+\nu)ker\ x - (4/x)(1+\nu)kei'\ x \\
-D_{4x} &= ker\ x - (2/x)kei'\ x \\
E_{4x} &= -xkei'\ x + 2(1+\nu)kei\ x + (4/x)(1+\nu)ker'\ x
\end{aligned} \tag{A7}$$

The angle change of the tangents at the points of application and in the directions of X_3 and X_4 due to unit load at X_k are given by

$$K\lambda^2\delta_{3,4k} = C_{1k}D_{1x} + C_{2k}D_{2x} + C_{3k}D_{3x} + C_{4k}D_{4x} \tag{A8}$$

where

$$K = Et^3/12(1 - \nu^2)$$

while the horizontal displacement of the cone boundary edges at and in the direction of loads X_1 and X_2 due to unit load at X_k are given by Hooke's law for middle surface deformation:

$$\delta_{1,2k} = (s\sin\alpha/Et)(N_\theta - \nu N_\phi) \tag{A9}$$

or

$$2Et\delta_{1,2k}/\sin\alpha\tan\alpha = C_{1k}E_{1x} + C_{2k}E_{2x} + C_{3k}E_{3x} + C_{4k}E_{4x}$$

As a check on the computation of Eqs. (8) and (9), Betti's

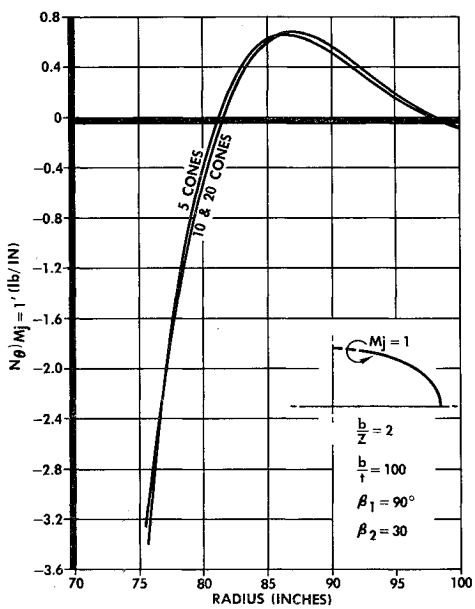

Fig. 3 Typical hoop load per inch distribution showing the effect of the number of approximating cones

Table 1 Influence coefficients: a comparison of the cone solution with Galletly's[3] and Clark's[3] solutions for a toroid with positive curvature with constant thickness (a = 230 in., b = 34.625 in., t = 1.25 in.)

Edge loading		β	Galletly	Clark	4 cones	15 cones
Unit moment at β = 73°	$E\delta_{24}$	73°	1007.0	990.0	971.49	975.80
	$E\delta_{14}$	36°10′	−695.7	−680.0	−675.70	−673.29
Unit inward horizontal force at β =73°	$E\delta_{22}$	73°	+11545.0	+11400.0	+11155.6	+11210.9
	$E\delta_{12}$	36°10′	−4554.0	−4375.0	−4446.8	−4424.6
Unit moment at β = 36°10′	$E\delta_{23}$	73°	+792.4	+776.0	+767.88	+771.76
	$E\delta_{13}$	36°10′	−834.3	−820.0	−826.24	−820.54
Unit outward horizontal force at β = 36°10′	$E\delta_{21}$	73°	−4343.0	−4180.0	−4232.6	−4211.4
	$E\delta_{11}$	36°10′	8657.0	8530.0	8477.2	8396.3
Unit moment at β = 73°	$E\delta_{44}$	73°	+134.2	+132.5	+130.6	+130.8
	$E\delta_{34}$	36°10′	+77.99	+76.2	+74.94	+75.27
Unit inward horizontal force at β = 73°	$E\delta_{42}$	73°	1007.0	987.0	971.49	975.80
	$E\delta_{32}$	36°10′	830.1	811.0	806.75	810.83
Unit moment at β = 36°10′	$E\delta_{43}$	73°	73.95	72.6	71.33	71.64
	$E\delta_{33}$	36°10′	138.7	137.6	137.5	137.8
Unit outward horizontal force at β = 36°10′	$E\delta_{41}$	73°	−664.0	−646.0	−643.14	−640.9
	$E\delta_{31}$	36°10′	−834.5	−818.0	−826.24	−820.54

Table 2 Influence coefficients: a comparison of the cone solution with Galletly's[4] solution for a shell of negative Gaussian curvature with constant thickness (b/t = 10, a/b = 7)

Edge loading	β		Galletly	5 cones		Galletly	5 cones
bX_1 = 1		$Eb^2\delta_{31}$	−2556.5	−2585.5	$Eb\delta_{11}$	1474.4	1480.3
X_3 = 1		$Eb^2\delta_{33}$	7747.5	7825.8	$Eb\delta_{13}$	−2556.5	−2585.5
$-bX_2$ = 1	β_1 = 90°	$Eb^2\delta_{32}$	1271.8	1301.6	$Eb\delta_{12}$	−471.72	−481.25
$-X_4$ = 1		$Eb^2\delta_{34}$	2140.8	2138.4	$Eb\delta_{14}$	−1651.4	−1634.8
bX_1 = 1		$Eb^2\delta_{41}$	−1469.9	−1455.0	$Eb\delta_{21}$	−419.87	−428.34
X_3 = 1	β_2 = 15°	$Eb^2\delta_{43}$	1905.4	1903.2	$Eb\delta_{23}$	1132.0	1158.5
$-bX_2$ = 1		$Eb^2\delta_{42}$	2084.5	2083.2	$Eb\delta_{22}$	1011.6	1042.9
$-X_4$ = 1		$Eb^2\delta_{44}$	9977.0	9691.2	$Eb\delta_{24}$	2084.5	2083.2

Table 3 Influence coefficients: a comparison of the cone solution with Galletly's[5] solution of an ellipsoidal shell with constant thickness (b/t = 100, b/z = 2)

Edge loading	β		Galletly	5 cones		Galletly	5 cones
$-X_2/t$ = 1		$E\delta_{42}$	334.34	333.37	$E/t\delta_{22}$	+2580.8	+2576.55
X_4/t^2 = 1		$E\delta_{44}$	+85.349	+85.228	$E/t\delta_{24}$	334.37	333.38
X_1/t = 1	β_1 = 90°	$E\delta_{41}$	+4.9803	+4.9817	$E/t\delta_{21}$	25.043	25.467
$-X_3/t^2$ = 1		$E\delta_{43}$	−0.68714	−0.68714	$E/t\delta_{23}$	−7.8585	−7.8737
$-X_2/t$ = 1		$E\delta_{32}$	−10.420	−10.416	$E/t\delta_{12}$	+33.181	+33.691
X_4/t^2 = 1		$E\delta_{34}$	−0.91900	−0.90903	$E/t\delta_{14}$	6.6024	6.5904
X_1/t = 1	β_2 = 30°	$E\delta_{31}$	−238.46	−246.23	$E/t\delta_{11}$	1232.1	1254.2
$-X_3/t^2$ = 1		$E\delta_{33}$	99.879	101.115	$E/t\delta_{13}$	−238.46	−246.23

reciprocal deflection theorem extended to line loads may be represented in the form[2]

$$c_i\delta_{ik} = c_k\delta_{ki} \tag{A10}$$

where c_i is the circumference at the X_i load, and δ_{ik} is the deformation at i, at and in the direction of $X_i = 1$, due to a unit load at k, i.e., $X_k = 1$. For the case considered, $c_1 = c_3 = s_1$ and $c_2 = c_4 = s_2$, since the circumference is proportional to the slant height.

To complete the solution, the following quantities are defined in terms of the Kelvin functions:

$$\begin{aligned} F_{1x} &= x\,ber'\,x - 2\,ber\,x + (4/x)bei'\,x \\ F_{2x} &= x\,bei'\,x - 2\,bei\,x - (4/x)ber'\,x \\ F_{3x} &= x\,ker'\,x - 2\,ker\,x + (4/x)kei'\,x \\ F_{4x} &= x\,kei'\,x - 2\,kei\,x - (4/x)ker'\,x \end{aligned} \tag{A11}$$

and

$$\begin{aligned} G_{1x} &= x\,bei'\,x + 2(1-\nu)[bei\,x + (2/x)ber'\,x] \\ -G_{2x} &= x\,ber'\,x + 2(1-\nu)[ber\,x - (2/x)bei'\,x] \\ G_{3x} &= x\,kei'\,x + 2(1-\nu)[kei\,x + (2/x)ker'\,x] \\ -G_{4x} &= x\,ker'\,x + 2(1-\nu)[ker\,x - (2/x)kei'\,x] \end{aligned} \tag{A12}$$

When the X_k loads are unity or a given value, the final solutions for the stress resultants at point x are given by superposition:

$$\begin{aligned} N_s &= -\frac{\tan\alpha}{S}\sum_{k=1}^{4} X_k \sum_{p=1}^{4} C_{pk}A_{px} \\ N_\theta &= -\frac{\tan\alpha}{S}\sum_{k=1}^{4} X_k \sum_{p=1}^{4} C_{pk}F_{px} \\ M_s &= \frac{2}{x^2}\sum_{k=1}^{4} X_k \sum_{p=1}^{4} C_{pk}B_{px} \\ M_\theta &= \frac{2}{x^2}\sum_{k=1}^{4} X_k \sum_{p=1}^{4} C_{pk}G_{px} \end{aligned} \tag{A13}$$

The values of stress resultants may be computed by means of Eq. (13) for different values of x along the shell and must satisfy the end conditions at the boundaries.

The method of coupling a series of cones together is shown in Appendix B. The extent of the general application of the conical-segment approximation to shells can be seen by examining the limiting cases of the cone equation, which are those for a flat plate with a hole in the center for one limit and that for a cylinder for the other limit.[7]

Table 4 Stress influence coefficients: a comparison of the conical segment method solution with Galletly's solution[10] for a torus

	$\phi = 90°$		$\phi = 75°$		$\phi = 60°$		$\phi = 45°$		$\phi = 30°$	
	$M\phi$	$bN\theta$	$M\phi$	$bN\theta$	$M\phi$	$bN\theta$	$M\phi$	$bN\theta$	$M\phi$	$bN\theta$
Galletly's solution										
$bH_1 = 1$	...	23.073	−0.03806	0.39219	−0.00218	−1.14090	0.00124	−0.13672	...	0.22840
$M_1 = 1$	1.0	−132.75	0.23789	26.705	−0.03541	8.0948	−0.01414	−0.69190	...	−1.6827
$bH_2 = 1$	...	−0.35630	−0.00191	0.49205	0.01227	1.5166	0.04760	−3.5544	...	−18.228
$M_2 = 1$	...	−3.0529	−0.03837	0.86552	−0.00148	21.518	0.50433	21.010	1.0	−212.01
Conical segment method solution										
$bH_1 = 1$	...	23.2066	−0.037487	0.32292	−0.002053	−1.1327	0.001233	−0.13103	...	0.22614
$M_1 = 1$	1.0	−134.974	0.23409	26.8922	−0.035588	8.0657	−0.013946	−0.71385	...	−1.6670
$bH_2 = 1$	...	−0.35335	−0.00188	0.48810	0.012127	1.52663	0.047511	−3.5734	...	−18.441
$M_2 = 1$	...	−2.9335	−0.037430	0.80105	−0.00366	21.269	0.49490	21.5588	1.0	−199.546

Table 5 Stress influence coefficients: a comparison of the conical segment method of solution with Galletly's solution[10] for an ellipsoid

	$\phi = 90°$		$\phi = 75°$		$\phi = 60°$		$\phi = 45°$		$\phi = 30°$	
	$M\phi/h^2$	$N\theta/h$	$M\phi/h^2$	$N\theta/h$	$M\phi/h^2$	$N\theta/h$	$M\phi/h^2$	$N\theta/h$	$M\phi/h^2$	$N\theta/h$
$H_3/h = 1$	...	−36.426	−3.0488	−3.7877	−0.41829	2.2710	0.12705	0.13478	...	0.00317
$M_3/h^2 = 1$	1.0	3.3236	0.38082	−0.56577	−0.02474	−0.33290	−0.01528	0.02589	...	−0.00764
$H_2/h = 1$	...	−0.000399	0.00898	0.05742	−0.07086	−0.05437	0.20106	−1.3283	...	22.589
$M_2/h^2 = 1$	...	−0.00757	0.00065	0.01182	−0.01269	0.02752	−0.03005	−0.28805	1.0	3.1996
Galletly's solution										
Conical segment method solution										
$H_3/h = 1$	0	−36.400	−3.0487	−3.7591	−0.41599	2.2699	0.12618	0.13182	...	0.000917
$M_3/h^2 = 1$	1.0	3.3197	0.38015	−0.5677	−0.02496	−0.3319	−0.01512	0.02593	....	−0.008053
$H_2/h = 1$	0	−0.0009489	−0.008952	0.05828	−0.07183	−0.05318	0.20421	−1.3524	...	22.926
$M_2/h^2 = 1$	...	−0.007618	0.000649	0.01196	−0.01287	0.02757	−0.02946	−0.2939	1.0	3.2865

Flat Plate

The form of Eq. (1) holds for a meridian angle change ϕ,[1] as well as for the shear force Qs; therefore, writing Eq. (1) in terms of ϕ,

$$0 = \left[S\frac{d^2\phi}{dS^2} + \frac{d\phi}{dS} - \frac{\phi}{S}\right] \pm i\,[12(1-\nu^2)]^{1/2}\frac{\cot\alpha}{t}\cdot\phi \quad \text{(A14)}$$

For a flat plate, in the limit, $\alpha \to \pi/2$, $\cot\alpha \to 0$, and $s \to r$, the plate radius; the equation becomes

$$r(d^2\phi/dr^2) + (d\phi/dr) - (\phi/r) = 0 \quad \text{(A15)}$$

which is the plate equation for a plate with zero transverse shear.[6]

Cylinder

The cylinder is the limiting case where the apex of the cone approaches infinity. Let $S = S_1 + x$, where S_1, the distance of the apex from the upper edge, $\to \infty$, and x is the variable $dS = dx$, and Eq. (14) becomes

$$\tan\alpha\left[(S_1+x)\frac{d^2\phi}{dx^2} + \frac{d\phi}{dx} - \frac{\phi}{S_1+x}\right] \pm i\,[12(1-\nu^2)]^{1/2}\frac{\phi}{t} = 0 \quad \text{(A16)}$$

In the limit as $\alpha \to 0$, $\tan\alpha \to 0$, but $\tan\alpha\,[(S_1+x)] \to a$, the cylindrical radius. Hence

$$a(d^2\phi/dx^2) \pm i[12(1-\nu^2)]^{1/2}(\phi/t) = 0 \quad \text{(A17)}$$

This is equivalent to the single equation

$$a^2(d^4\phi/dx^4) + 12(1-\nu^2)(\phi/t^2) = 0 \quad \text{(A18)}$$

Since $\phi = dw/dx$, the meridian angle change,

$$\frac{d}{dx}\left[\frac{d^4w}{dx^4} + \frac{12(1-\nu^2)}{a^2t^2}w\right] = 0 \quad \text{(A19)}$$

This is the equation of a cylinder.[6]

Appendix B

Coupling the Cones

The method of coupling the cones will be illustrated by coupling the top cone j to the next cone $j-1$ beneath it. For continuity of the two cone segments, see Fig. 1 at the joint:

$$\Sigma F = 0 = X_{2_j} + X_{i-1} \quad \text{(B1)}$$

$$\Sigma M = 0 = X_{4_j} + X_{3_{j-1}} \quad \text{(B2)}$$

$$\Sigma\Delta_{j \text{ and } j-1} = 0 = X_{1_j}\delta_{21_j} + X_{2_j}\delta_{22_j} + X_{3_j}\delta_{23_j} + X_{4_j}\delta_{24_j} - X_{1_{j-1}}\delta_{11_{j-1}} - X_{2_{j-1}}\delta_{12_{j-1}} - X_{3_{j-1}}\delta_{13_{j-1}} - X_{4_{j-1}}\delta_{14_{j-1}} \quad \text{(B3)}$$

$$\Sigma\theta_{j \text{ and } j-1} = 0 = X_{1_j}\delta_{41_j} + X_{2_j}\delta_{42_j} + X_{3_j}\delta_{43_j} + X_{4_j}\delta_{44_j} - X_{1_{j-1}}\delta_{31_{j-1}} - X_{2_{j-1}}\delta_{32_{j-1}} - X_{3_{j-1}}\delta_{33_{j-1}} - X_{4_{j-1}}\delta_{34_{j-1}} \quad \text{(B4)}$$

For the end cone, known external end loads are substituted into the equations such that $X_{3_j} = M_j$ and $X_{1_j} = P_j$. The other cones are coupled in a similar manner, resulting in a matrix equation from which the unknown edge loads X_2 and X_4 can be determined for each cone. Using the general relations derived from Eqs. (B1) and (B2), the unknown X_1 and X_3 loads can be evaluated from

$$X_{2_{j-n+2}} = -X_{1_{j-n+1}} \qquad X_{4_{j-n+2}} = -X_{3_{j-n+1}} \quad \text{(B5)}$$

The matrix solution for X_2 and X_4 is of the form

$$[H]^T[X_{2,4}] = [X\delta]$$

where for $2(j-1)$ terms

$$[X\delta] = \begin{bmatrix} -\delta_{21_j} & 0 & -\delta_{23_j} & 0 \\ -\delta_{41_j} & 0 & -\delta_{43_j} & 0 \\ 0 & 0 & 0 & 0 \\ 0 & 0 & 0 & 0 \\ \cdot & \cdot & \cdot & \cdot \\ \cdot & \cdot & \cdot & \cdot \\ 0 & \delta_{12_{j-n}} & 0 & \delta_{14_{j-n}} \\ 0 & \delta_{32_{j-n}} & 0 & \delta_{34_{j-n}} \end{bmatrix} \begin{bmatrix} P_j \\ P_1 \\ M_j \\ M_1 \end{bmatrix}$$

and

$$[\mathrm{H}]^T = \begin{bmatrix} |A|_0 & |B| & |J| & |J| \\ |C|_1 & |A|_1 & |B|_2 & |J| \\ |J| & |C|_2 & |A|_2 & |B|_3 \\ |J| & |J| & |C|_3 & |A|_3 \end{bmatrix}$$

where

$$|A|_a = \begin{bmatrix} (\delta_{22_{j-a}} + \delta_{11_{j-a-1}})(\delta_{24_{j-a}} + \delta_{13_{j-a-1}}) \\ (\delta_{42_{j-a}} + \delta_{31_{j-a-1}})(\delta_{44_{j-a}} + \delta_{33_{j-a-1}}) \end{bmatrix}$$

$$|B|_a = \begin{bmatrix} -\delta_{12_{j-a}} - \delta_{14_{j-a}} \\ -\delta_{32_{j-a}} - \delta_{34_{j-a}} \end{bmatrix}$$

$$|C|_a = \begin{bmatrix} -\delta_{21_{j-a}} - \delta_{23_{j-a}} \\ -\delta_{41_{j-a}} - \delta_{43_{j-a}} \end{bmatrix}$$

$$|J| = \begin{bmatrix} 0 & 0 \\ 0 & 0 \end{bmatrix}$$

The matrix unknown X_2 and X_4 loads are evaluated for the unit load case where the known shell end loads $X_{1_{jI}}$, $X_{3_{jIII}}$, $X_{2_{j-n_{II}}}$, $X_{4_{j-n_{IV}}}$ are equal to 1 or 0 each in turn. The form of $X_{2,4}$ is therefore

$$[X_{2,4}] = \begin{bmatrix} X_{2_{j_I}} & X_{2_{j_{II}}} & X_{2_{j_{III}}} & X_{2_{j_{IV}}} \\ X_{4_{j_I}} & X_{4_{j_{II}}} & X_{4_{j_{III}}} & X_{4_{j_{IV}}} \\ X_{2_{j-1_I}} & X_{2_{j-1_{II}}} & X_{2_{j-1_{III}}} & X_{2_{j-1_{IV}}} \\ X_{4_{j-1_I}} & X_{4_{j-1_{II}}} & X_{4_{j-1_{III}}} & X_{4_{j-1_{IV}}} \\ \cdot & \cdot & \cdot & \cdot \\ \cdot & \cdot & \cdot & \cdot \\ \cdot & \cdot & \cdot & \cdot \\ \cdot & \cdot & \cdot & \cdot \\ X_{2_{j-n+1_I}} & X_{2_{j-n+1_{II}}} & X_{2_{j-n+1_{III}}} & X_{2_{j-n+1_{IV}}} \\ X_{4_{j-n+1_I}} & X_{4_{j-n+1_{II}}} & X_{4_{j-n+1_{III}}} & X_{4_{j-n+1_{IV}}} \end{bmatrix}$$

from which the unknown X_2 and X_4 and, therefore, X_1 and X_3 loads can be found for each cone. Using these evaluated loads, the stress distribution for each cone segment can be determined from Eq. (13).

The deflection influence coefficient matrix for their reassembled shell can be determined from the matrix equation:

$$[\delta] = [\bar{D}][\bar{E}] \tag{B6}$$

where

$$[\bar{D}] = \begin{bmatrix} \delta_{11_j} & \delta_{12_j} & \delta_{13_j} & \delta_{14_j} & 0 & 0 & 0 & 0 \\ 0 & 0 & 0 & 0 & \delta_{21_{j-n}} & \delta_{22_{j-n}} & \delta_{23_{j-n}} & \delta_{24_{j-n}} \\ \delta_{31_j} & \delta_{32_j} & \delta_{33_j} & \delta_{34_j} & 0 & 0 & 0 & 0 \\ 0 & 0 & 0 & 0 & \delta_{41_{j-n}} & \delta_{42_{j-n}} & \delta_{43_{j-n}} & \delta_{44_{j-n}} \end{bmatrix}$$

and

$$[\bar{E}] = \begin{bmatrix} 1 & 0 & 0 & 0 \\ X_{2_{i_I}} & X_{2_{i_{II}}} & X_{2_{i_{III}}} & X_{2_{i_{IV}}} \\ 0 & 0 & 1 & 0 \\ X_{4_{i_I}} & X_{4_{i_{II}}} & X_{4_{i_{III}}} & X_{4_{i_{IV}}} \\ X_{1_{j-n_I}} & X_{1_{j-n_{II}}} & X_{1_{j-n_{III}}} & X_{1_{j-n_{IV}}} \\ 0 & 1 & 0 & 0 \\ X_{3_{j-n_I}} & X_{3_{j-n_{II}}} & X_{3_{j-n_{III}}} & X_{3_{j-n_{IV}}} \\ 0 & 0 & 0 & 1 \end{bmatrix}$$

and the deflection influence coefficient matrix, for the whole reassembled shell being analyzed, is

$$[\delta] = \begin{bmatrix} \delta_{11} & \delta_{12} & \delta_{13} & \delta_{14} \\ \delta_{21} & \delta_{22} & \delta_{23} & \delta_{24} \\ \delta_{31} & \delta_{32} & \delta_{33} & \delta_{34} \\ \delta_{41} & \delta_{42} & \delta_{43} & \delta_{44} \end{bmatrix} \tag{B7}$$

The reciprocal relation used for the individual cone [Eq. (A10)], also applies to the deflection influence coefficients of the whole reassembled shell.

Comparison of Stress Influence Coefficients

It was brought to the authors' attention that a tabulation of stress influence coefficients had been published by Galletly[10] for several shells. Tables 4 and 5 show a comparison between Galletly's results and solutions for the same shells obtained by the conical segment method. It can be seen that good agreement was obtained.

References

[1] Flugge, W., *Statik und Dynamik der Schalen* (Springer-Verlag, Berlin, 1957), 2nd ed., pp. 192–200.

[2] Love, A. E. H., *A Treatise on the Mathematical Theory of Elasticity* (Dover Publications Inc., New York, 1944), 4th ed., p. 173.

[3] Galletly, G. D., "A comparison of methods for analyzing bending effects in toroidal shells," J. Appl. Mech. **25**, 413–414 (September 1958).

[4] Galletly, G. D., "Edge influence coefficients for toroidal shells of negative Gaussian curvature," J. Eng. Ind. **82**, 69–75 (1960).

[5] Galletly, G. D., "Bending of 2:1 and 3:1 open crown ellipsoidal shells," Welding Research Council Bull. 54 (October 1959).

[6] Timoshenko, S. and Woinowsky-Krieger, S., *Theory of Plates and Shells* (McGraw-Hill Book Co. Inc., New York, 1959), 2nd ed., pp. 53, 468.

[7] Dubois, F., *Uber die Festigkeit der Kegelschale* (Zurich Eidgenossischen Technischen Hochschule, Zurich, 1917), pp. 52–56.

[8] Baltrukonis, J. H., "Influence coefficients for edge loaded short, thin conical frustums," Space Technology Labs. Rept. EM 8-2 (January 30, 1958).

[9] Clark, R. A., "On the theory of thin elastic toroidal shells," J. Math. Phys. **29**, 146–178 (1950).

[10] Galletly, G. D., "Influence coefficients and pressure vessel analysis," J. Eng. Ind. **B82**, 259–269 (August 1960).